Supporting Information

Insights into the effect of donor ability on photophysical properties of dihydroindeno[2,1-c]fluorene-based imide derivatives

Guiying He,[ab] Li-Li Zhou,[b] Hongwei Song,[ab] Zhuoran Kuang,[ab] Xian Wang,[ab] Qianjin Guo,[a] Hai-Yan Lu*[b] and Andong Xia*[ab]

[a.] *Beijing National Laboratory for Molecular sciences (BNLMS), Key Laboratory of Photochemistry, Institute of Chemistry, Chinese Academy of Sciences, Beijing 100190, People's Republic of China. E-mail: andong@iccas.ac.cn*

[b.] *University of Chinese Academy of Sciences, Beijing 100049, People's Republic of China. E-mail: haiyanlu@ucas.ac.cn*

S1. Synthesis and characterization of imide dyes

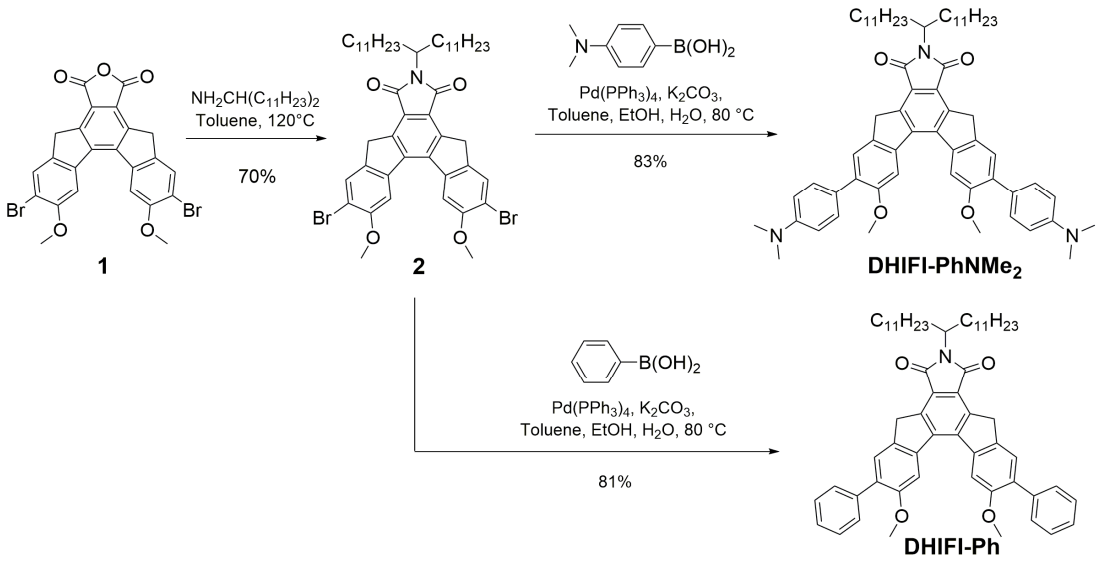

Scheme S1 Chemical structures of **DHIFI-PhNMe$_2$** and **DHIFI-Ph** and their synthetic routes.

3,11-Dibromo-7-(tricosan-12-yl)-2,12-dimethoxy-5*H*-diindeno-[2,1-*e*:1′,2′-*g*]isoindole-6,8(7*H*,9*H*)-dione (2): To a solution of compound **1** (539 mg, 1 mmol) in toluene (50 mL) under argon was added tricosan-12-amine (1017 mg, 3 mmol), and the mixture was stirred at 120°C for 24h. The reaction mixture was cooled to room temperature, dried over anhydrous $MgSO_4$, and then concentrated under reduced pressure. The residue was purified by flash column chromatography with dichloromethane : petroleum ether (1:3, *v*/*v*) as eluent to afford compound **2** (603 mg, 70%) as pale yellow powder. ^{1}H NMR (500 MHz, $CDCl_3$): δ 8.00 (s, 2H), 7.86 (s, 2H), 4.25 (s, 4H), 4.17-4.23 (m, 1H), 4.03 (s, 6H), 2.15–2.04 (m, 2H), 1.77–1.69 (m, 2H), 1.35–1.12 (m, 36H), 0.84 (t, J = 7.0 Hz, 6H). ^{13}C NMR (125 MHz, $CDCl_3$): δ 169.2, 155.3, 141.9, 141.8, 140.5, 139.4, 130.4, 124.8, 113.3, 107.6, 57.0, 52.5, 35.0, 32.7, 32.0, 29.8, 29.7, 29.6, 29.5, 26.9, 22.8, 14.3, 14.2. HR-MS (APCI): *m/z* calcd for $[M + H]^+$: 862.3040, found: 862.3031.

3,11-Bis(4-(dimethylamino)phenyl)-7-(tricosan-12-yl)-2,12-dimethoxy-5*H*-diindeno[2,1-*e*:1′,2′-*g*]isoindole-6,8(7*H*,9*H*)-dione (DHIFI-PhNMe$_2$): To a mixture of compound **2** (86 mg，0.1 mmol), (4-(dimethylamino)phenyl)boronic acid (495 mg，0.3 mmol) in toluene (24 mL), ethanol (16 mL) and H_2O (8 mL) under argon atmosphere was added catalytic amount of $Pd(PPh_3)_4$ (14 mg, 0.012 mmol). The mixture was stirred at 80 ℃ for 24 hours under argon atmosphere, cooled to room temperature, and then added dichloromethane (100 mL) and water (50 mL). The organic layer was dried over anhydrous $MgSO_4$, and then concentrated under reduced pressure. The residue was purified by column chromatography with ethyl acetate : petroleum ether (0.3:2, *v*/*v*) as eluent to give compound **DHIFI-PhNMe$_2$** (78 mg, 83%) as orange red power. ^{1}H NMR (500 MHz, $CDCl_3$): δ 8.18 (s, 2H), 7.64 (s, 2H), 7.56 (d, *J* = 8.7 Hz, 4H), 6.83 (d, *J* = 8.6 Hz, 4H), 4.30 (s, 4H), 4.23 (tt, *J* = 10.1, 5.2 Hz, 1H), 3.96 (s, 6H), 3.01 (s, 12H), 2.17–2.08 (m, 2H), 1.78–1.69 (m, 2H), 1.37–1.16 (m, 36H), 0.85 (t, *J* = 7.0 Hz, 6H). ^{13}C NMR (125 MHz, $CDCl_3$): δ 169.6, 156.2, 149.9, 142.5, 142.2, 139.6, 138.7, 132.1, 130.4, 127.1, 126.1, 123.9, 112.3, 107.7, 56.6, 52.3, 40.7, 35.3, 32.8, 32.0, 29.8, 29.71, 29.65, 29.6, 29.50, 29.47, 27.0, 22.8, 14.25. HR-MS (APCI): *m/z* calcd for $[M + H]^+$: 944.6300, found: 944.6304.

7-(tricosan-12-yl)-2,12-dimethoxy-3,11-diphenyl-5*H*-diindeno-[2,1-*e*:1′,2′-*g*]isoindole-6,8(7*H*,9*H*)-dione (DHIFI-Ph): After a mixture of compound **2** (86 mg, 0.1 mmol), phenylboronic acid (366 mg, 0.3 mmol) and K_2CO_3 (138 mg, 1 mmol) in toluene (24 mL), ethanol (16 mL) and H_2O (8 mL) was kept under argon atmosphere, catalytic amount of $Pd(PPh_3)_4$ (14 mg, 0.012 mmol) was added. The mixture was stirred at 80 °C for 24h under argon atmosphere, cooled to room temperature and then poured into dichloromethane (100 mL) and water (50 mL). The organic phase was separated, dried over anhydrous $MgSO_4$ and concentrated under reduced pressure to give a residue, which was purified by column chromatography with dichloromethane : petroleum ether (1:4, *v*/*v*) as eluent to afford compound **DHIFI-Ph** (69 mg, 81%) as pale yellow powder. ^{1}H NMR (500 MHz, $CDCl_3$): δ 8.20 (s, 2H), 7.66 (s, 2H), 7.63 (d, *J* = 7.3 Hz, 4H), 7.46 (t, *J* = 7.6 Hz, 4H), 7.37 (t, *J* = 7.4 Hz, 2H), 4.32 (s, 4H), 4.23 (tt, *J* = 10.1, 5.2 Hz, 1H), 3.96 (s, 6H), 2.18–2.06 (m, 2H), 1.82-1.68 (m, 2H), 1.38–1.14 (m, 36H), 0.84 (t, *J* = 6.9 Hz, 6H). ^{13}C NMR (125 MHz, $CDCl_3$): δ 169.5, 156.2, 142.5, 142.3, 140.6, 138.6, 132.0, 129.7, 128.3, 127.7, 127.5, 124.3, 107.6, 56.6, 52.3, 35.3, 32.8, 32.04, 29.762, 29.756, 29.71, 29.65, 29.49, 29.47, 27.0, 22.8, 14.2. HR-MS (APCI): *m/z* calcd for $[M + H]^+$: 858.5456, found: 858.5456.

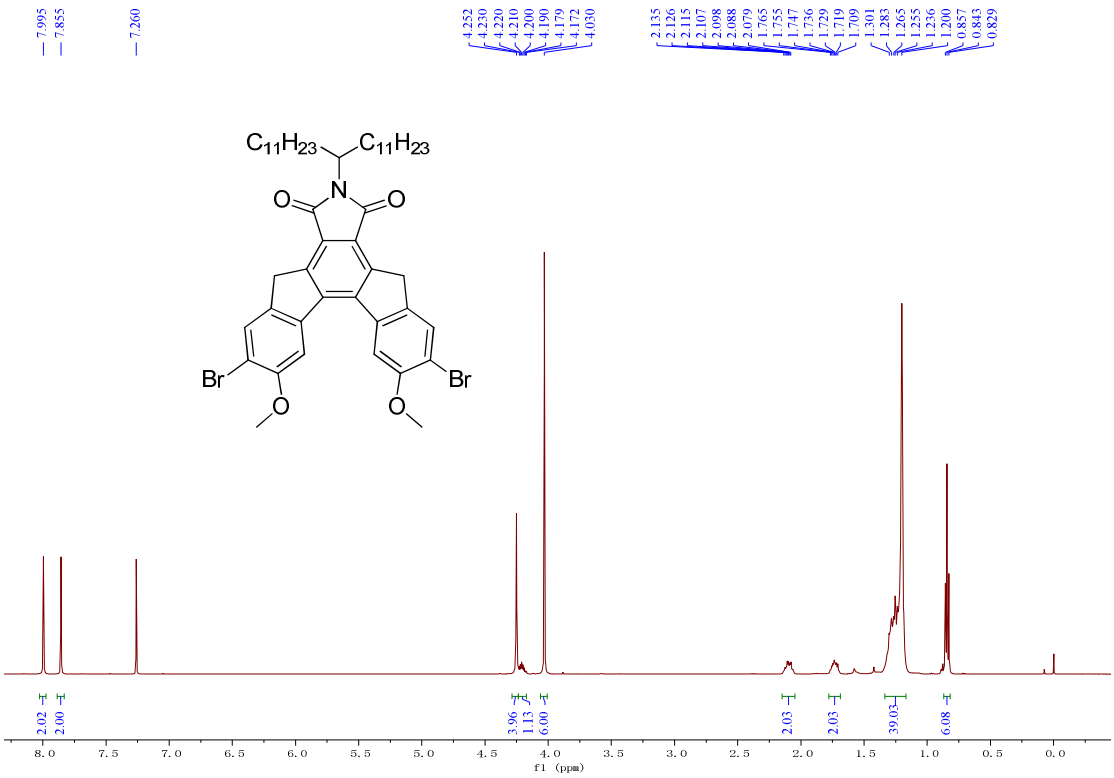

Fig. S1 ^{1}H NMR spectrum (500 MHz, $CDCl_3$) of **2**.

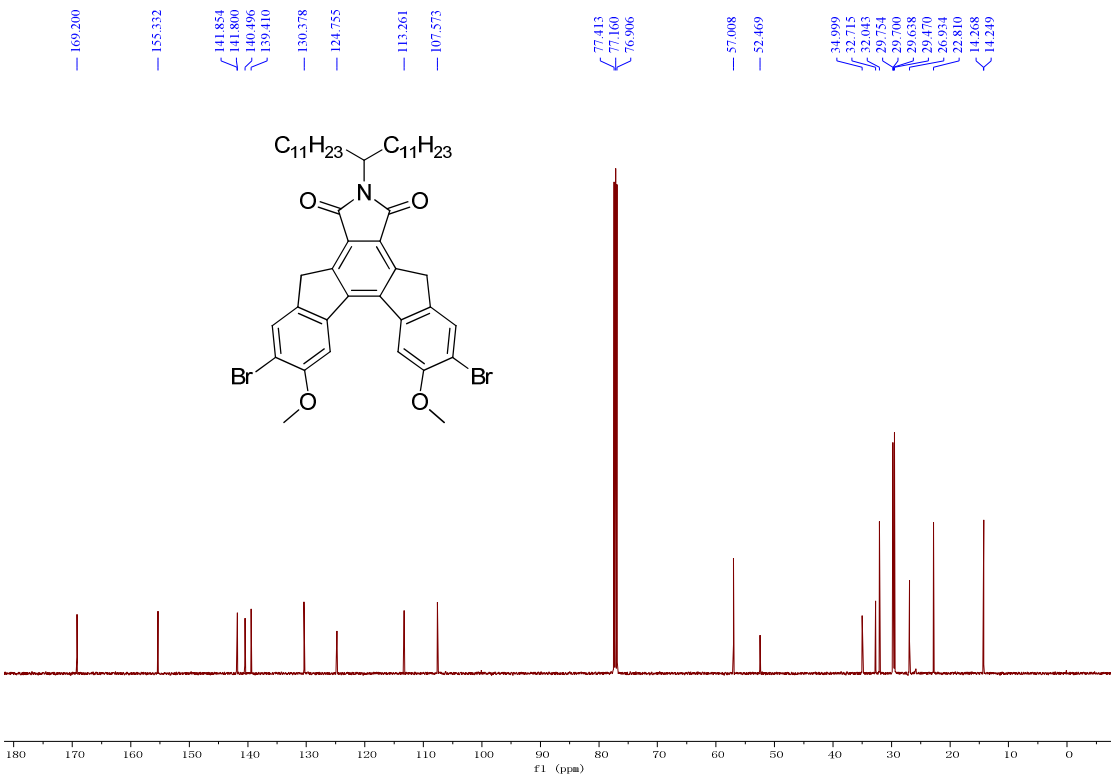

Fig. S2 ^{13}C NMR spectrum (125 MHz, $CDCl_3$) of **2**.

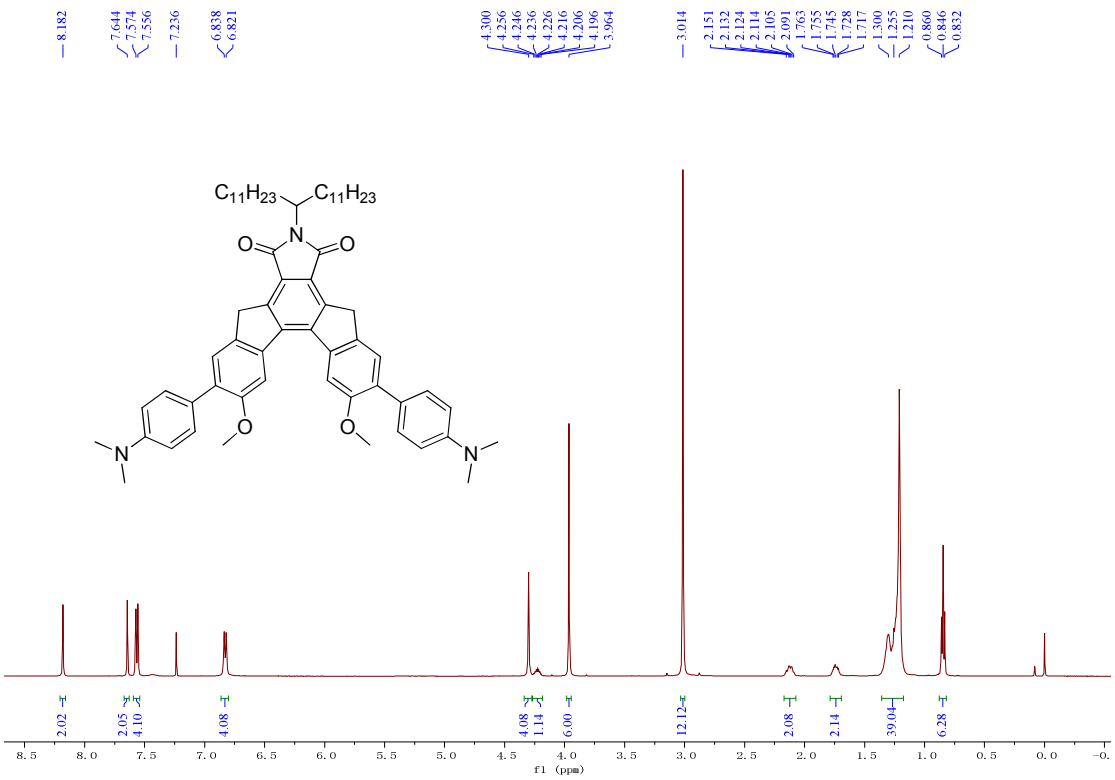

Fig. S3 ^{1}H NMR spectrum (500 MHz, $CDCl_3$) of **DHIFI-PhNMe$_2$**.

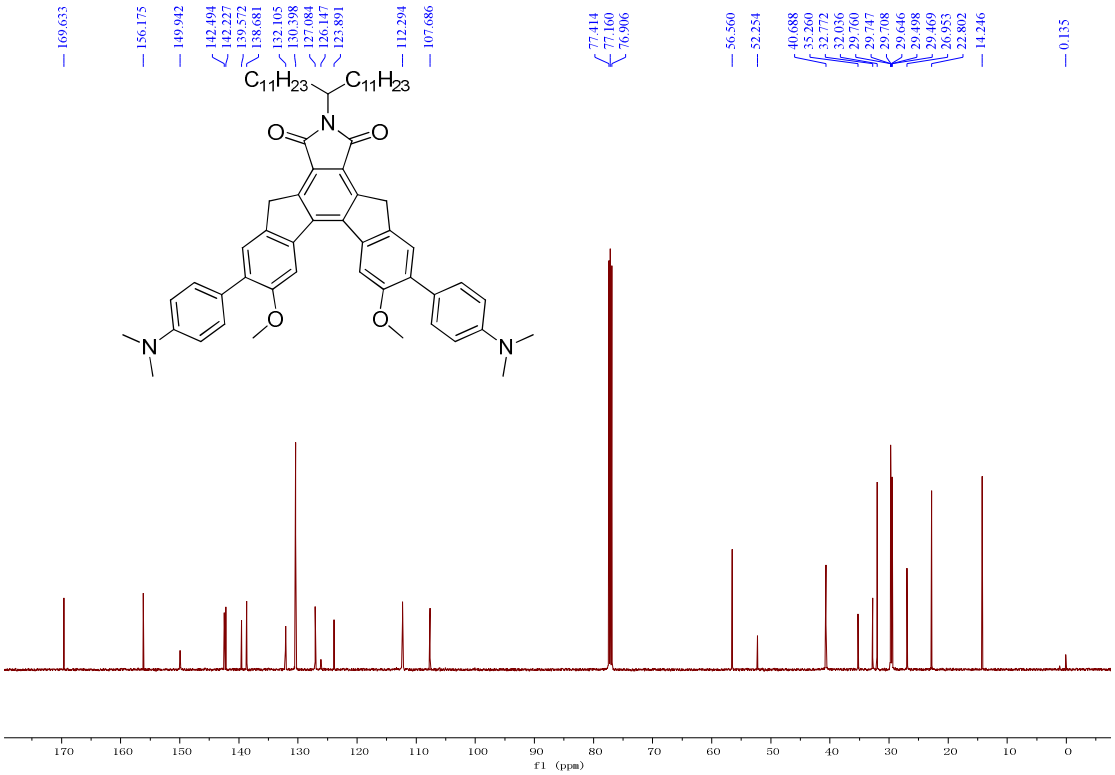

Fig. S4 ^{13}C NMR spectrum (125 MHz, $CDCl_3$) of **DHIFI-PhNMe$_2$**.

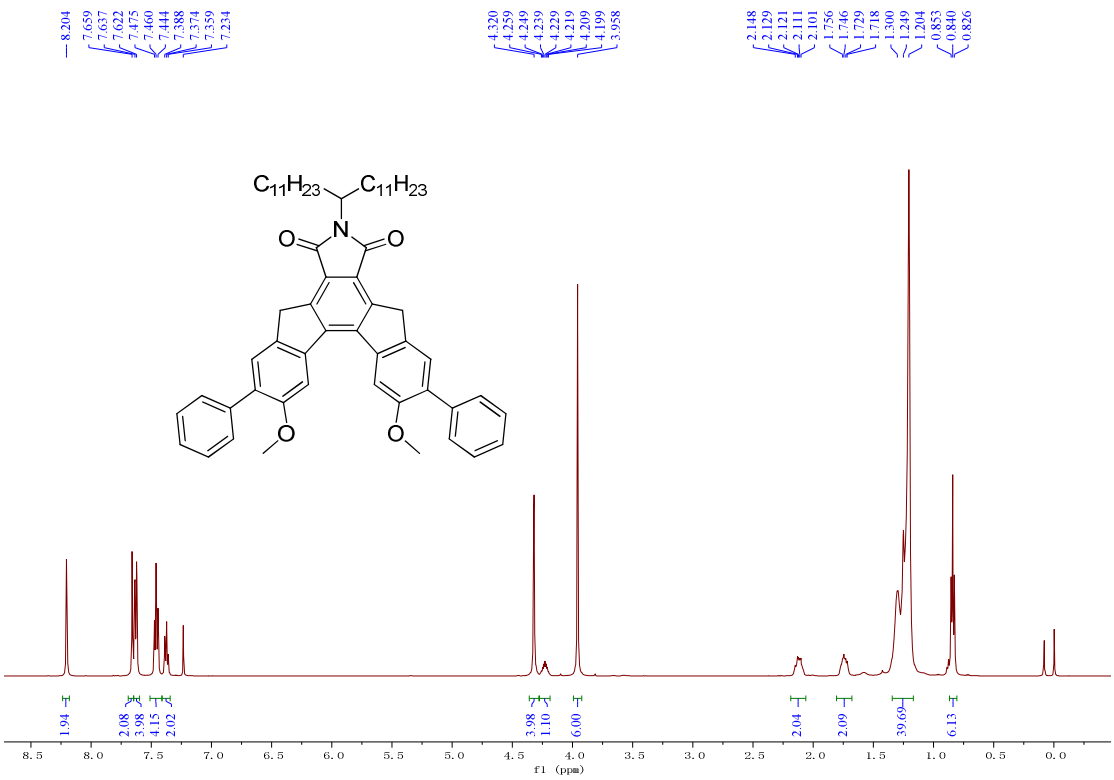

Fig. S5 ^{1}H NMR spectrum (500 MHz, $CDCl_3$) of **DHIFI-Ph**.

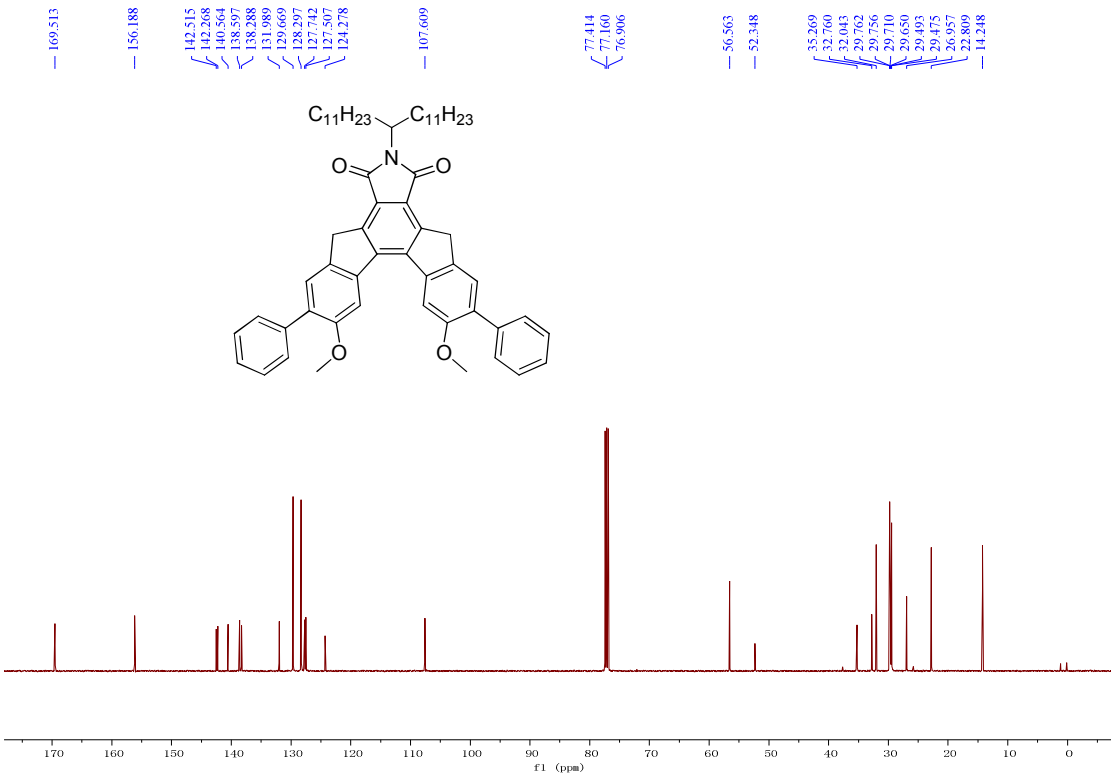

Fig. S6 ^{13}C NMR spectrum (125 MHz, $CDCl_3$) of **DHIFI-Ph**.

S2. Solvation effects on fluorescence quantum yield and lifetime

As shown in Table 1, the fluorescence properties are sensitive to the polarity of solvents. Fig. S7 shows the

fluorescence lifetimes of dye **DHIFI-PhNMe2** and **DHIFI-Ph** in different solvents by time-correlated single photon counting (TCSPC) measurements.

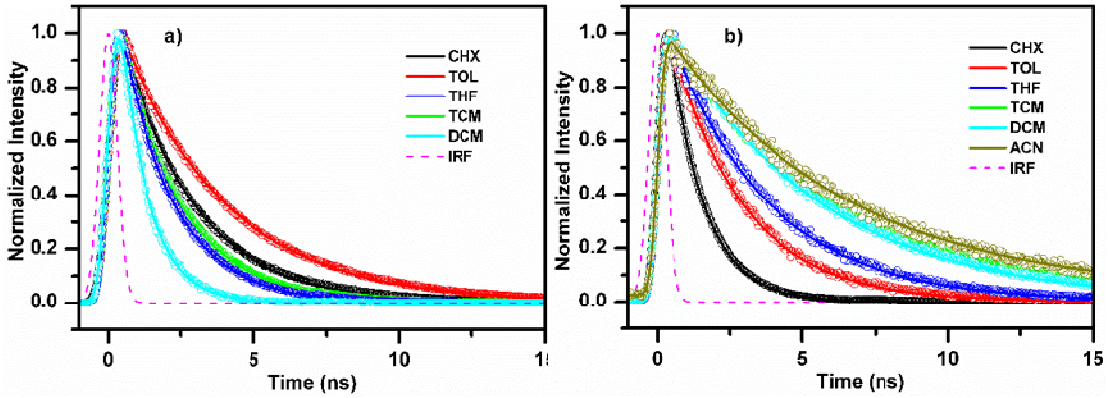

Fig. S7 Fluorescence lifetimes of dyes, (a) **DHIFI-PhNMe2** and (b) **DHIFI-Ph**. Fitting results are also included.

The radiative and nonradiative rate constants k_r and k_{nr} are calculated from the measured Φ and τ_f as based on equation S1 and S2:

$$k_r = \Phi_f / \tau_f \quad \text{(S1)}$$

$$k_{nr} = 1/\tau_f - k_r \quad \text{(S2)}$$

The radiative rate k_r decreases with the increasing polarity. While for **DHIFI-PhNMe2**, the nonradiative rate k_{nr} increases deeply in polar solvents.

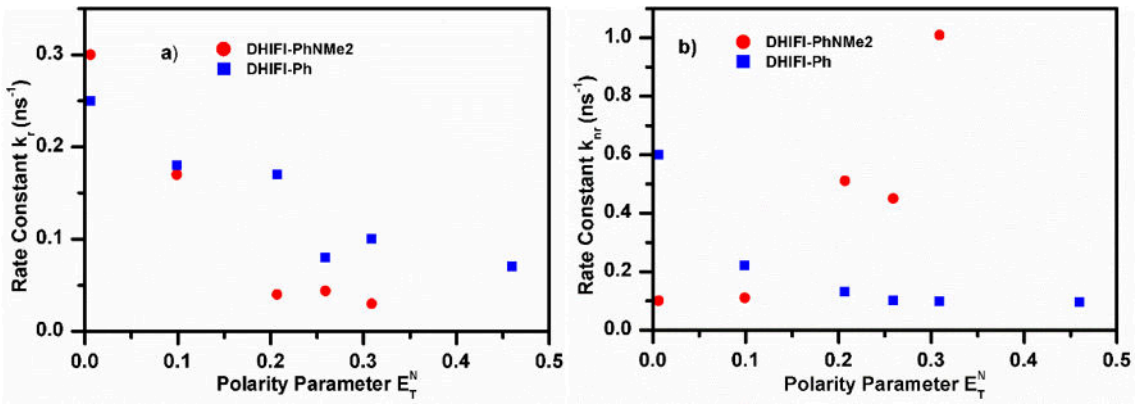

Fig. S8 Plots of reactive decay rate constants (a) and nonradiative decay rate constants against solvent polarity.

S3. Molecular frontier orbitals of dyes

The molecular frontier orbitals of dyes are shown in Fig. S9. It is found that the similar LUMO orbitals located on the dihydroindeno[2,1-c]fluorene core. However, the HOMOs are quite different. A key character is bigger contribution of dimethylamine to the HOMO for **DHIFI-PhNMe2**, which demonstrated the strong donor ability. The transition energy of the lowest excited state are shown here. Small energy gap of **DHIFI-PhNMe2** must result from the strong donor-acceptor ability.

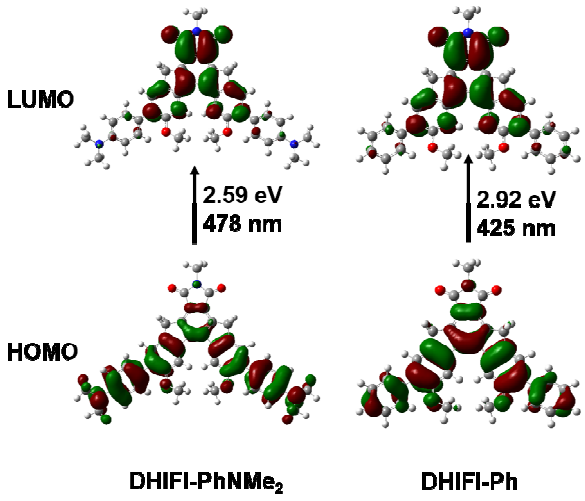

Fig. S9 The frontier molecular orbitals based on the optimized structure. The transition energy of the lowest excited state shown here.

S4. The optimized structures and dipole moment determination of dyes

The structure model of dihydroindeno[2,1-c]fluorene backbone are shown in Fig. S10. The small dihedral α indicated more planar structure. The calculated dihedrals of α and β (β') indicates the geometry relaxation of excited states. Furthermore, dipole moments of excited state and oscillator strength of absorption and emission were obtained by TD-DFT method (shown in Fig. S11 and S12).

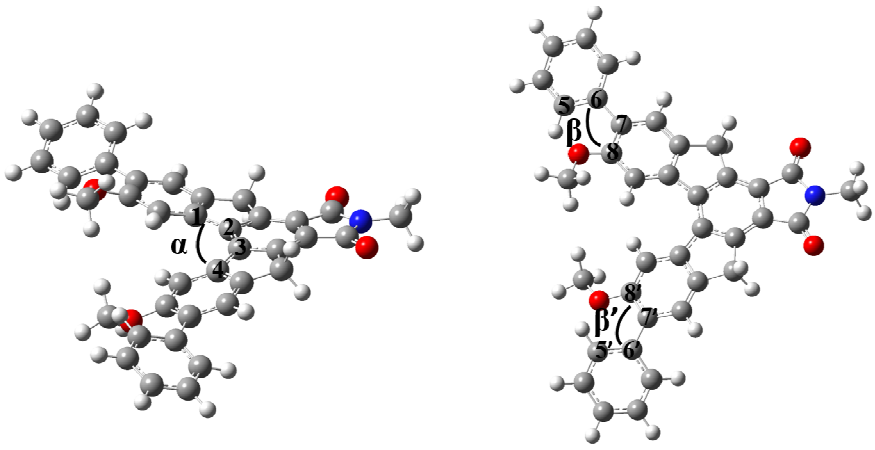

Fig. S10 The optimized structures of dyes. α , β (β') are the dihedral angle.

Table S1 The dihedral angle of the optimized ground and excited state structures.

	Ground state			Excited state		
	α	β	β'	α	β	β'
DHIFI-PhNMe$_2$	13.47	45.12	45.09	20.27	36.70	36.74
DHIFI-Ph	14.07	47.35	47.34	22.62	39.86	39.87

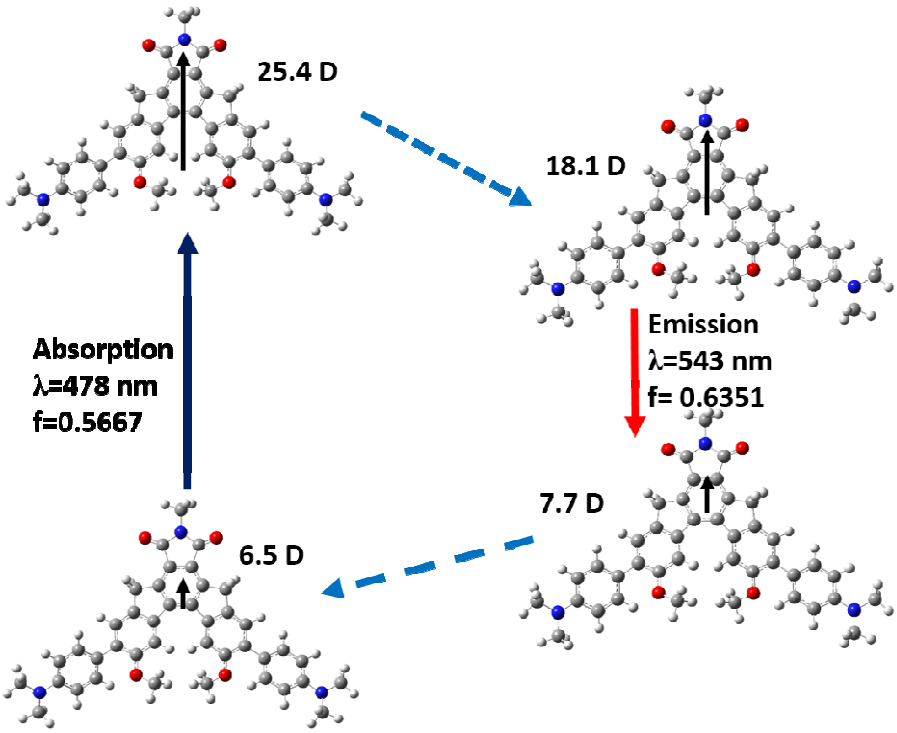

Fig. S11 The optimized structures and their dipole moment for **DHIFI-PhNMe2** are shown along with energies and oscillator strengths of absorption and emission.

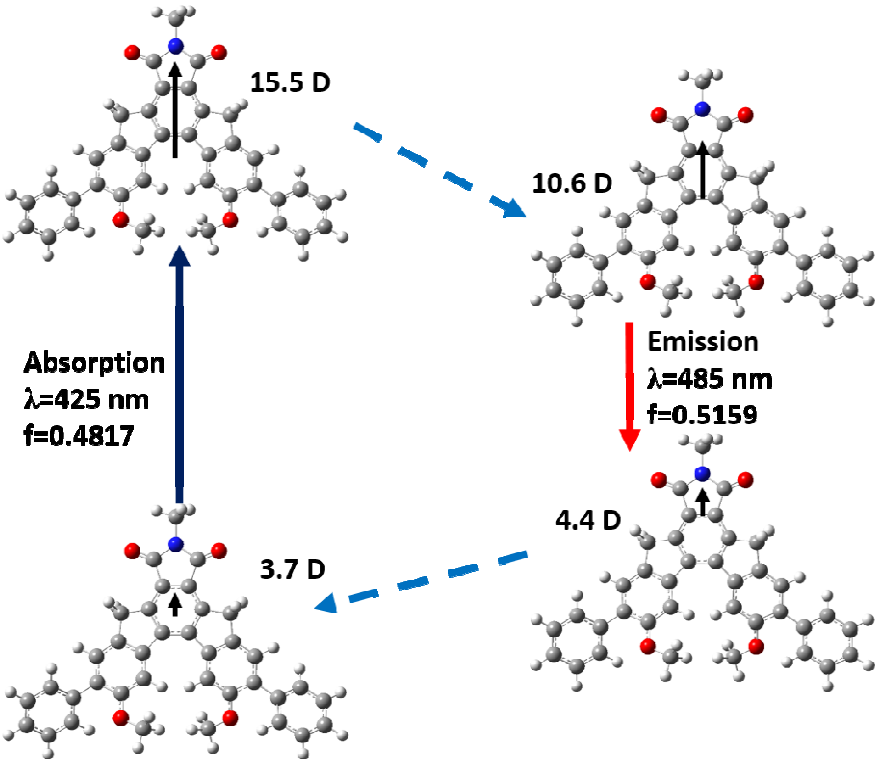

Fig. S12 The optimized structures and their dipole moment for **DHIFI-Ph** are shown along with energies and oscillator strengths of absorption and emission.

S5. The global analyses of transient absorption spectra of DHIFI-Ph

Fig. S13 shows the kinetics of selected wavelengths in TOL and THF. It is observed that the same dynamics of ESA around 550 nm and 690 nm. At the delay of around 200 ps, the ESA around 440 nm increases with the decay of other two ESA bands.

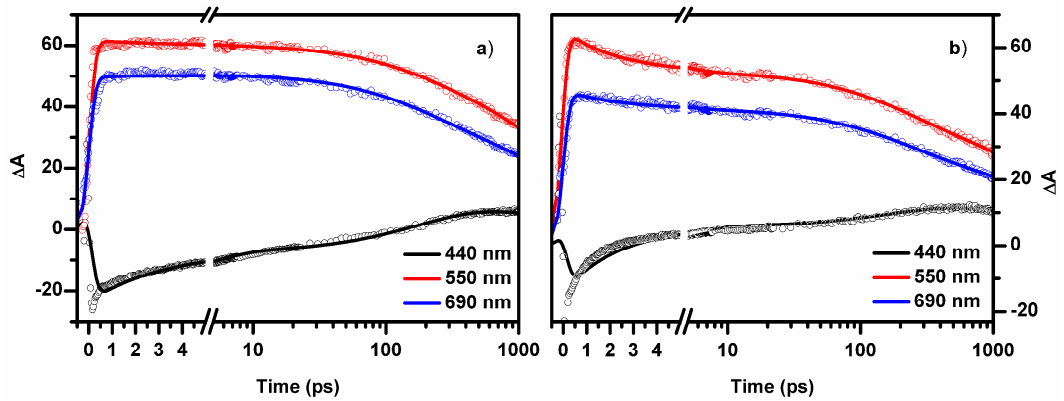

Fig. S13 The kinetics of selected wavelengths of **DHIFI-Ph** in TOL (a) and THF (b).

To extract the dynamics of **DHIFI-Ph** in TOL and THF, global analysis with a sequential model were carried out. Fig. S14 shows the EADS and corresponding population evolution.

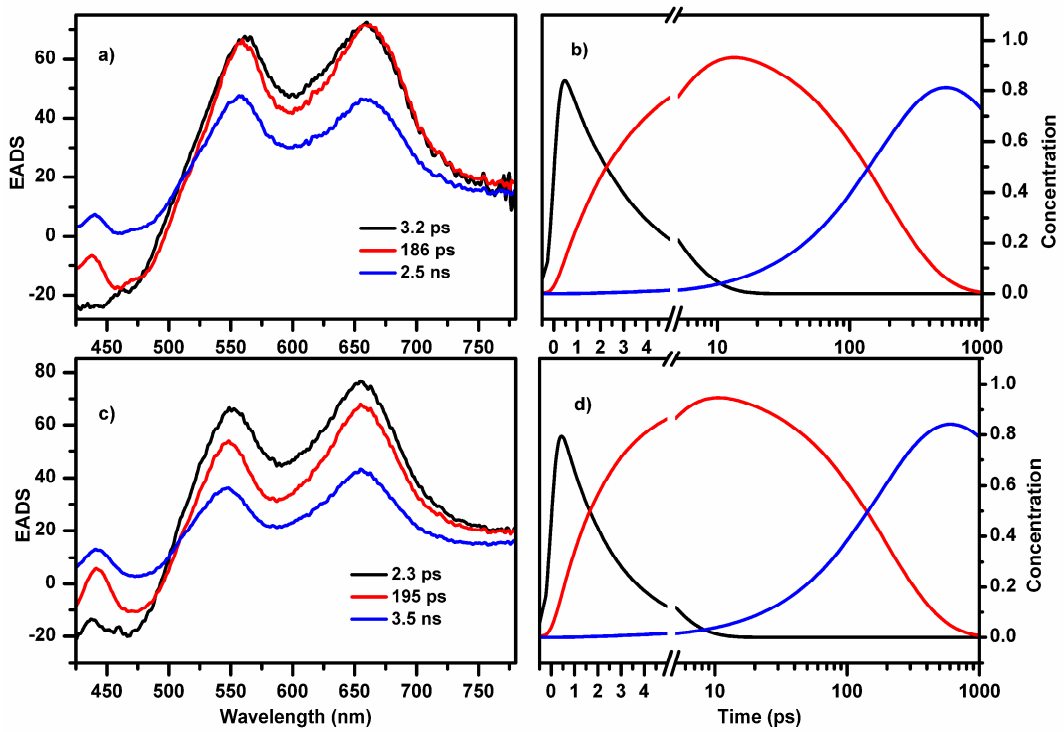

Fig. S14 Global analysis of the transient absorption spectra. EADS obtained by a sequential model for **DHIFI-Ph** in TOL (a) and THF (c), corresponding population evolution shown (b, d).

S6. Nanosecond transient spectra by flash photolysis

The nanosecond transient spectra of dyes in THF are shown in Fig. S15, which display the similar evolution with that in TOL as the description in text. To testify the triplet, the measurements of air- and N_2-saturated solution were also carried out. The kinetics (probe at 500 nm for **DHIFI-PhNMe2** and 550 nm for **DHIFI-Ph**) shown in Fig. S16 to demonstrate the prolonged lifetime in N_2-saturated solution.

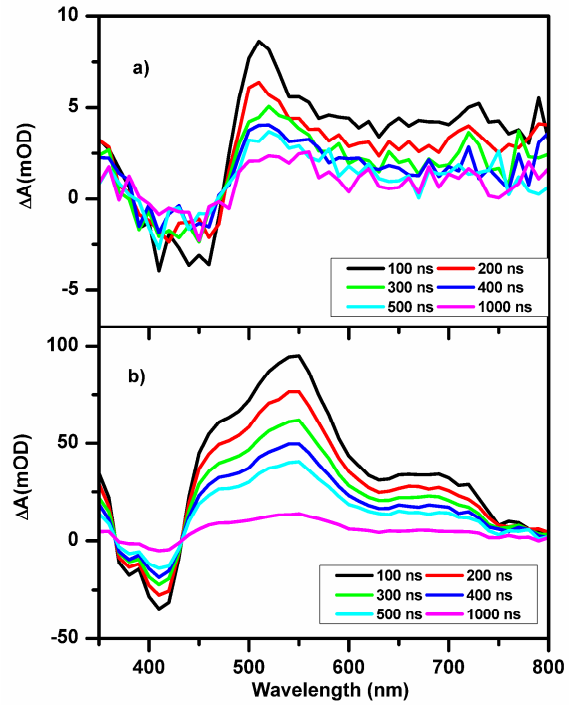

Fig. S15 Nanosecond time-resolved transient spectra of **DHIFI-PhNMe2** (a) and **DHIFI-Ph** (b) in THF.

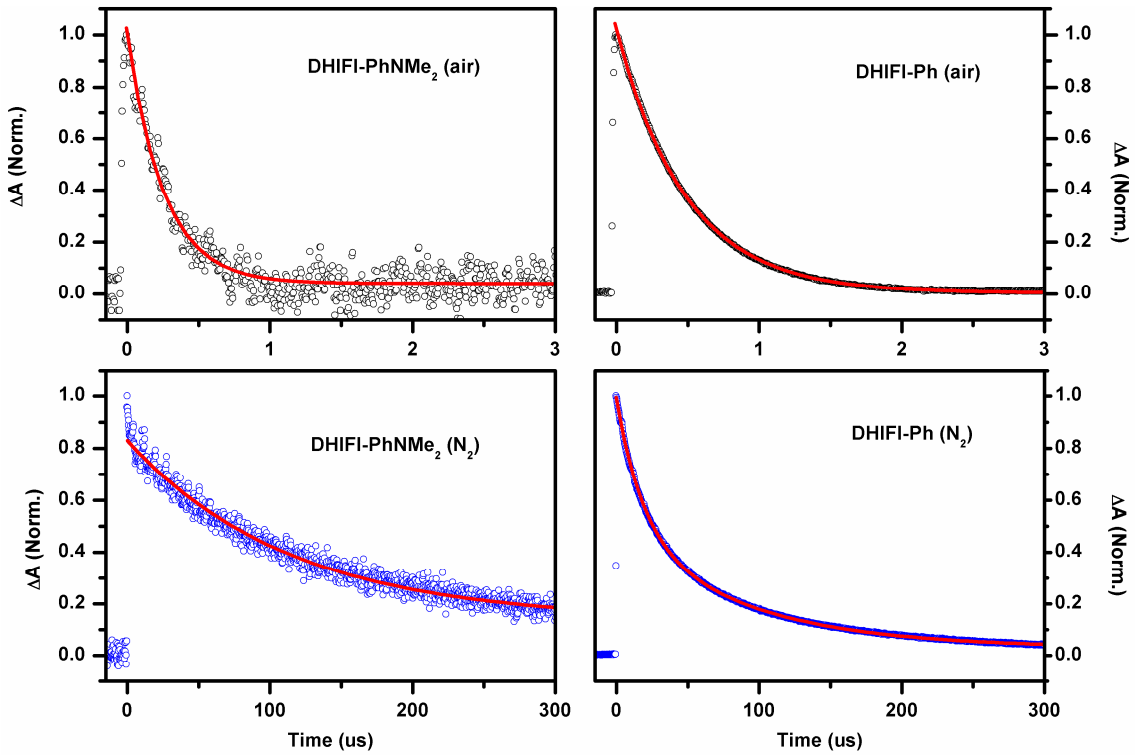

Fig. S16 The kinetic trace of **DHIFI-PhNMe2** and **DHIFI-Ph** in air and N_2 saturated TOL.

To determine the triplet state quantum yields by ISC, time-resolved singlet oxygen phosphorescence detection in the near-IR (1270 nm) were recorded. Experimentally, the singlet oxygen quantum yield can be given by the following equation:

$$\int_0^\infty S_t dt = S_0 \times \frac{\tau_\Delta}{\tau_\Delta - \tau_T} \int_0^\infty [\exp(-t/\tau_\Delta) - \exp(-t/\tau_\Delta)]dt$$
$$= S_0 \times \tau_\Delta = \kappa k_{\Delta,R} [^1PS^*]_0 \times \Phi_\Delta \tau_\Delta \quad \text{(S3)}$$

where the time-integrated signals is proportional to factor of setup (κ), radiative decay of singlet oxygen ($k_{\Delta,R}$), the concentration of excited singlet species ($[^1PS^*]_0$), the quantum yield (Φ_Δ) and lifetime (τ_Δ) of singlet oxygen. Thus, the calculated triplet state yield is obtained by following equation:

$$\Phi_{\Delta,sample} = \Phi_{\Delta,ref} \times \frac{S_{ss,sample}}{S_{ss,ref}} \times \frac{(\kappa k_{\Delta,R} I_{abs} \tau_\Delta)_{ref}}{(\kappa k_{\Delta,R} I_{abs} \tau_\Delta)_{sample}} \quad \text{(S4)}$$

Table S2. Parameters from singlet phosphorescence detection in 1270 nm

	solvents	Integrate S	I_{abs} (OD)	$k_{\Delta,R}$	τ_Δ (us)	Φ_Δ
DHIFI-PhNMe2	TOL	7.9×10^7	0.3152	0.98	37.7	0.105
	THF	3.0×10^7	0.3417	0.52	27.7	0.093
DHIFI-Ph	TOL	15.3×10^7	0.3301	0.98	35.2	0.233
	THF	6.7×10^7	0.2971	0.52	27.1	0.220
Phenalenone	D_2O	20.0×10^7	0.2824	0.12	92	0.98

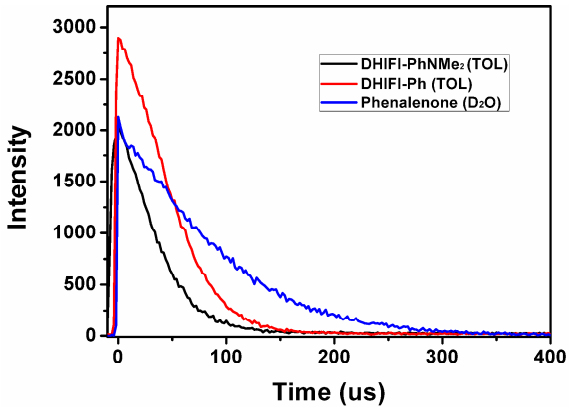

Fig. S17 The decay curves of singlet $^1O_2$ of dyes in TOL and Phenalenone in D_2O.

S7. Excitation spectra of **DHIFI-PhNMe2** in THF

Fluorescence excitation spectra monitored at blue side around 590 nm and red side around 750 nm of fluorescence spectrum were recorded to determine the emissive state. Normalized absorption spectra are also shown in Fig. S18 for comparison. It is found the excitation spectra are almost the same as absorption spectrum, indicating that there is only one emission state.

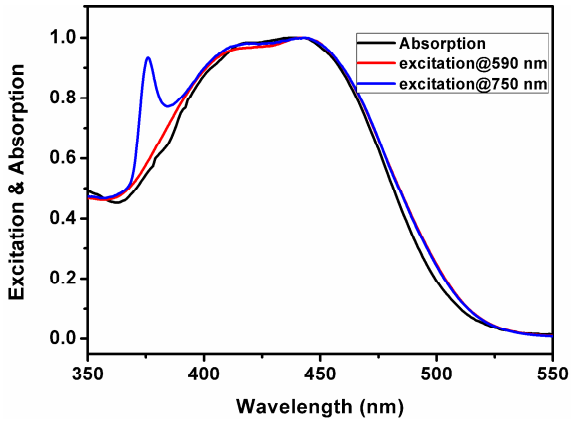

Fig. S18 Excitation spectra and absorption spectra of **DHIFI-PhNMe$_2$** in THF. The sharp peak around 375 nm is double frequency of 750 nm because of diffraction of grating.